



Crystal growth and 570 nm emission of Dy³⁺ doped CeF₃ single crystal

Yilun Yang^{a,b}, Lianhan Zhang^a, Shanming Li^{a,b}, Shulong Zhang^{a,b}, Peixiong Zhang^c, Mingzhu He^a, Min Xu^a, Yin Hang^{a,*}

^a Key Laboratory of High Power Laser Materials, Shanghai Institute of Optics and Fine Mechanics, Chinese Academy of Sciences, Shanghai, 201800, China

^b Center of Materials Science and Optoelectronics Engineering, University of Chinese Academy of Sciences, Beijing, 100049, China

^c Department of Optoelectronic Engineering, Jinan University, Guangzhou, 510632, China

ABSTRACT

A Dy³⁺-doped CeF₃ yellow region laser crystal was successfully grown using the Bridgman method. A 570 nm emission in Dy:CeF₃ crystal was observed for the first time. By analyzing the absorption and emission measurements of the Dy:CeF₃ crystal with the Judd–Ofelt theory, the intensity parameters $\Omega_{2,4,6}$, excited state lifetimes, branching ratios, and emission cross-sections were calculated. It is found that the Dy:CeF₃ crystal has high emission cross section ($0.9259 \times 10^{-20} \text{ cm}^2$) and long fluorescence lifetime (1.53 ms) corresponding to the stimulated emission of Dy³⁺:⁴F_{9/2} → ⁶H_{13/2} transition. We propose that the Dy:CeF₃ crystal may be a promising material for 570 nm laser applications.

1. Introduction

The continuous development of laser medicine, biomedical instruments, telecommunication, and many other fields, is leading visible lasers operating around yellow region have attracted much attention in view in the last years [1–3]. Regrettably, there is still a blank region in this band for LD, this puts forward requirements for the emission of yellow light laser by rare earth ion doped lasers. Among various rare earth activated ions, Dy³⁺ activated materials have attracted much attention due to the ⁴F_{9/2} to ⁶H_{13/2} transition luminescence emission [4]. The large energy gap between the ⁴F_{9/2} and next lower level ⁶F_{1/2} reduced multi-phonon relaxation [5]. Furthermore, the ⁴I_{15/2} dysprosium manifold near 450 nm and the continuous development of commercially available blue laser-diodes (LD) supplies with a new optical pump band [6]. These reasons make Dy³⁺ has great potential in yellow region visible laser applications. Recently, there have been many reports confirming the potential of Dy³⁺ on yellow light lasers, the output power and efficiency are also continuously improving [7–9].

The fluoride crystals attracted much attention in the search for new visible laser crystal hosts. Compared with oxide hosts, fluoride material possesses its combination of lower reflective index, good thermal properties, easy-processing, excellent solubility for rare-earth ions, and broadband transmittance from UV to mid-IR region [10,11]. Furthermore, the fluoride hosts have significantly lower maximum phonon energy (about 380 cm⁻¹) than other crystals [12], which is beneficial for suppressing multiphonon de-excitation processes. LaF₃ and CeF₃ crystals are such kind of materials that follow all the above advantages. LaF₃ single crystal is a well-known laser host and recently it has

attracted considerable interest for rare-earth ions doping [13,14]. Compared with LaF₃, its ionic radius is closer to rare earth activated ions, which makes it easier to dope. However, few works have studied the rare-earth ion doped CeF₃ crystal. On the basis of the above reasons, we made a systematic investigation on the Dy³⁺ doped CeF₃ single crystal.

In this work, the XRD patterns, IR transmittance spectrum, absorption spectrum, fluorescence spectrum and fluorescence decay curve of Dy:CeF₃ crystal have been recorded at room temperature. The J-O theory was used to analyze the absorption spectrum. The emission probability, fluorescence branching ratio radiation lifetime were calculated. Among them, the Dy³⁺:⁴F_{9/2} level fluorescence lifetime longer than other host crystals has attracted our attention. On the basis, systematically confirmed Dy:CeF₃ has great potential in yellow region visible laser emission.

2. Experimental section

The Dy³⁺ (2.0 at. %) single doped was grown by the Bridgman method. The CeF₃ (99.99%) and DyF₃ (99.99%) fluoride powder provided commercially have been used as raw materials. The raw material is packed into a 30 mm diameter graphite crucible, then spontaneously crystallize according to the set procedure. The melt in the crucible was melted for 10 h in the high-temperature zone with a temperature of 1360 °C. Then the crucible was pulled down to the low-temperature zone at the speed of 1.2 mm/h and a rotation rate of 5 rpm to drive the growth process. At last, the as grown crystal was cooled to room temperature at the rate of 30 °C/h. In order to avoid oxidation during

* Corresponding author.

E-mail address: yhang@siom.ac.cn (Y. Hang).

<https://doi.org/10.1016/j.jlumin.2019.116707>

Received 29 April 2019; Received in revised form 2 August 2019; Accepted 15 August 2019

Available online 16 August 2019

0022-2313/ © 2019 Elsevier B.V. All rights reserved.

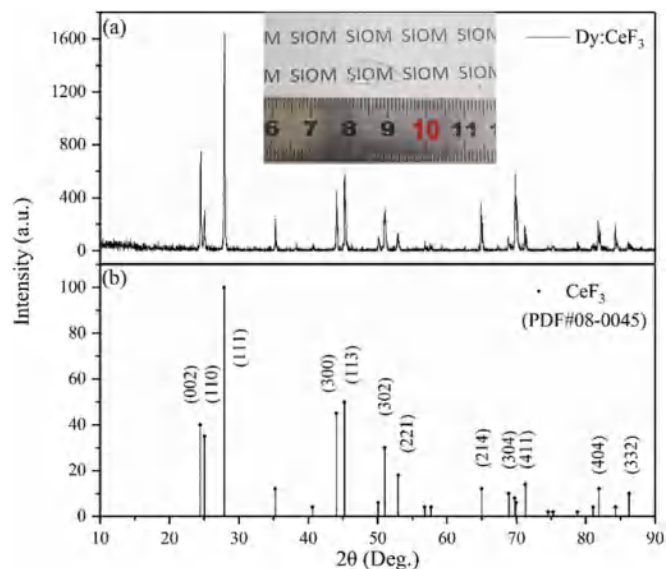


Fig. 1. The cutting sample and XRD pattern of CeF₃ crystals, (a) Dy:CeF₃ crystal and (b) CeF₃ crystal (JCPDS 08-0045).

crystal growth, the inside of the furnace was under the atmosphere of high-purity Argon (70%) and Carbon tetra-fluoride (30%) during the whole procedure. Finally, we got Dy:CeF₃ single crystal with size $\Phi 20 \text{ mm} \times 35 \text{ mm}$ size.

Crystal structure identification was undertaken on a D/max 2550 X-ray diffraction (XRD) using Cu K α radiation. The concentration of the Dy³⁺ ions was measured by inductively coupled plasma atomic emission spectrometry (ICP-AES) analysis. The IR transmittance spectrum of Dy:CeF₃ crystal was measured by Nicolet 6700 FTIR spectrometer. The absorption spectrum in the range of 300–2000 nm was recorded by a PerkinElmer Lambda 950 spectrometer. The fluorescence spectrum in range of 450–800 nm was measured under 350 nm xenon lamp pumping.

3. Results and discussions

The as-grown Dy:CeF₃ crystal was prepared successfully without any bubbles. The (100) oriented crystal sample is shown in Fig. 1, we can observe that the crystal is well crystallized and transparent. The doping concentrations of crystal sample for testing were measured to be 1.72 at.% of Dy³⁺. The segregation coefficient of Dy³⁺ in the CeF₃ crystal are approximate 0.82.

The XRD patterns of the Dy:CeF₃ crystal and the standard pattern of CeF₃ (JCPDS 08-0045), are shown in Fig. 2. In addition, the lattice parameters of Dy:CeF₃ was calculated to be $a = 0.7128 \text{ nm}$ and $c = 0.7284 \text{ nm}$, both very similar to pure CeF₃ single crystal ($a = 0.7112 \text{ nm}$, $c = 0.7279 \text{ nm}$). From the comparison we can find the diffraction peaks are strong and no second phase diffraction peak is found, indicating that the essential structure does not change while doped with rare-earth ions.

The infrared transmittance spectrum of Dy:CeF₃ crystal was measured at room temperature shown in Fig. 2. There is a wide absorption band in the region of 2.5–6.5 μm . One of the reasons for this phenomenon is because of the OH⁻ groups caused by fluoride absorbs water, which resulting in the absorption band region from 2.5 to 4 μm [15], the other reason is due to ²F_{7/2}-²F_{5/2} transition of Ce³⁺ [16]. The low transmittance in the mid-infrared band makes it very difficult to measure the fluorescence lifetimes of ⁶H_{13/2} energy level of Dy³⁺.

The room-temperature absorption spectra in the range of 300–2000 nm of Dy:CeF₃ crystal was shown as absorption cross-section in Fig. 3. There are 7 main absorption bands centered at around 348, 364, 802, 906, 1110, 1276 and 1694 nm, which correspond to the

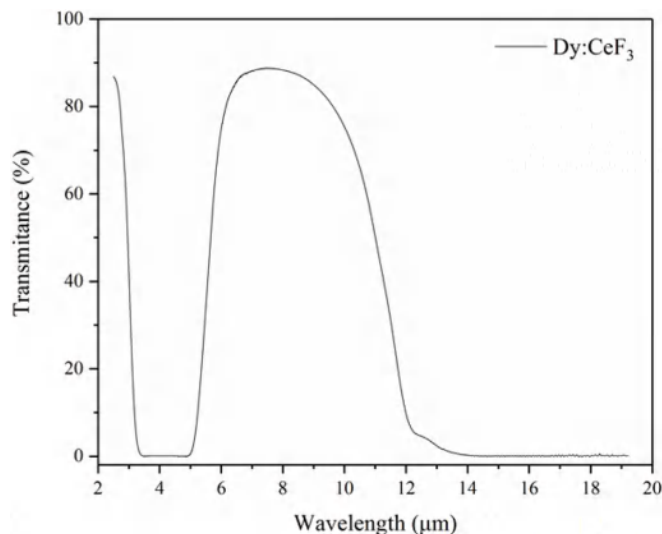


Fig. 2. Infrared transmittance spectrum of Dy:LaF₃ crystal.

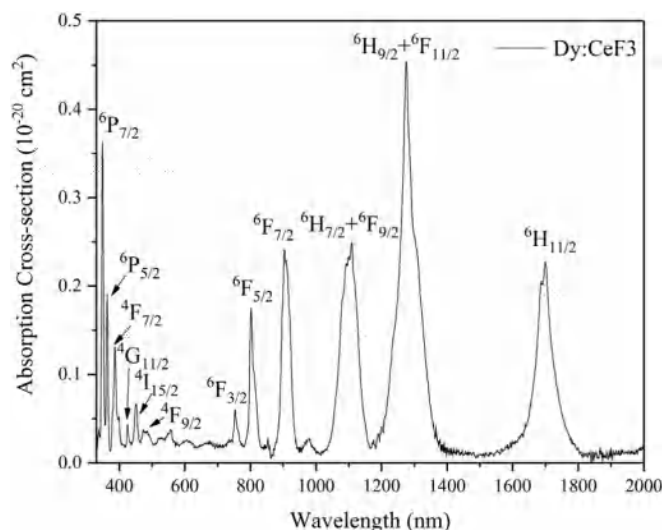


Fig. 3. Absorption cross-section of Dy:CeF₃ in the range of 300–2000 nm.

transitions starting from the ⁶H_{15/2} ground state to higher levels ⁶P_{7/2}, ⁶P_{5/2}, ⁶F_{5/2}, ⁶F_{7/2}, ⁶H_{7/2}+⁶F_{9/2}, ⁶H_{9/2}+⁶F_{11/2} and ⁶H_{11/2}, respectively [17]. The absorption bands centered at 450 nm are assigned to the ⁶H_{15/2} → ⁴I_{15/2} transition, which make this crystal suitable to be pumped by commercially available blue LDs [18], this increases the commercial potential of Dy³⁺ ions in visible lasers. The absorption cross-section could be calculated by the following formula:

$$\sigma_{\text{abs}}(\lambda) = \frac{2.303 \times OD(\lambda)}{L \times N_0} \quad (1)$$

where OD(λ) is the measured absorption optical density as a function of wavelength, L is the thickness of sample and N₀ is the number of Dy³⁺ ions per cm³. At the wavelength of 450 nm, the absorption cross-sections is $0.0661 \times 10^{-20} \text{ cm}^2$. Therefore, the Dy:CeF₃ crystal to be appropriate for commercial LD solid state laser pumping. The absorption peak, full bandwidth at half-maximum (FWHM), σ_{abs} , are listed in Table 1.

According to the absorption spectrum, the intensity parameters $\Omega_{2,4,6}$ of Dy³⁺ from the Judd-Ofelt theory were calculated. Judd-Ofelt theory [19,20] is widely applied to the study of electron transitions within the 4f shell of rare-earth ions in laser crystals. The detailed calculating process of J-O analysis is given in the following. The

Table 1
Central wavelengths, peak absorption cross-sections, and measured and calculated line strengths of Dy:CeF₃ crystal.

⁶ H _{15/2} to	λ (nm)	FWHM (nm)	σ _{abs} (10 ⁻²⁰ cm ²)	S _{mea} (10 ⁻²⁰ cm ²)	S _{cal} (10 ⁻²⁰ cm ²)
⁶ H _{11/2}	1694	64.9	0.2835	0.7664	0.7082
⁶ H _{9/2} + ⁶ F _{11/2}	1276	56.1	0.6142	1.6956	1.7016
⁶ H _{7/2} + ⁶ F _{9/2}	1110	55.5	0.3631	0.9407	1.0507
⁶ F _{7/2}	906	29.6	0.3908	0.8157	0.7441
⁶ F _{5/2}	802	18.1	0.1977	0.2531	0.3145
⁶ F _{3/2}	754	9.2	0.0534	0.0414	0.0557
⁴ F _{9/2}	472	6.9	0.0293	0.0483	0.0274
⁴ I _{15/2}	450	9.4	0.0661	0.0722	0.0698
⁴ G _{11/2}	426	4.9	0.0422	0.0298	0.0107
⁴ F _{7/2}	386	6.5	0.1262	0.1688	0.0778
⁶ F _{5/2}	364	5.6	0.2191	0.2139	0.0656
⁶ P _{7/2}	348	6.0	0.4155	0.4544	0.3610

Table 2
The Judd–Ofelt intensity parameters, ⁴F_{9/2} fluorescence lifetime and the concentration of the Dy³⁺ ions of Dy³⁺-doped crystals.

Crystals	Ω ₂ (10 ⁻²⁰ cm ²)	Ω ₄ (10 ⁻²⁰ cm ²)	Ω ₆ (10 ⁻²⁰ cm ²)	τ _f (μs)	Concentration (at. %)	Reference
Dy:YAG	0.20	1.11	1.46	911	5	[23]
Dy:GGG	0.17	2.66	2.57	790	2	[24]
Dy:YAP	3.93	1.64	3.79	185	3.46	[25]
Dy: CaGdAlO ₄	1.80	1.00	0.50	222	3	[26]
Dy:YVO ₄	6.59	3.71	1.74	310	1	[27]
Dy:LiYF ₄	2.01	1.34	2.39	–	–	[28]
Dy:LiLuF ₄	2.04	0.91	1.09	582	5	[29]
Dy:BaY ₂ F ₈	1.52	2.33	3.67	1240	0.5	[30]
Dy:PbF ₂	3.18	1.16	2.27	–	–	[31]
Dy:LaF ₃	1.75	1.94	1.97	1370	2	[32]
Dy:CeF ₃	1.01	0.69	0.91	1530	1.72	This work

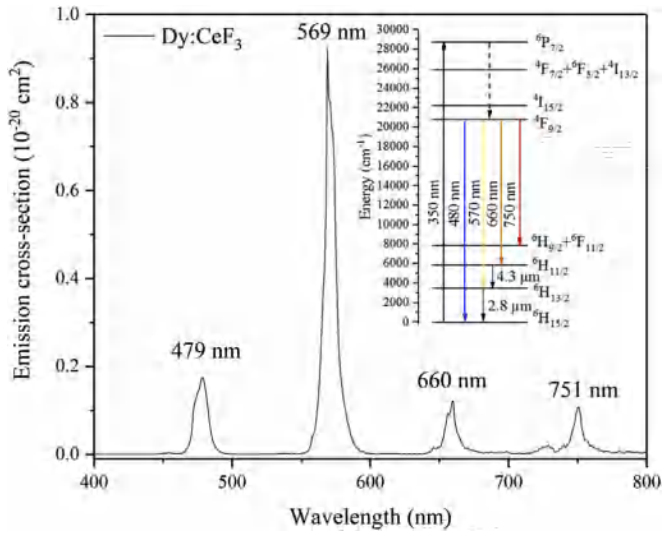


Fig. 4. Fluorescence emission cross-section and the energy level scheme of Dy:CeF₃ crystal.

experimental line strength S_{exp} can be calculated by the following equation:

$$S_{\text{exp}}(J, J') = \frac{3hc(2J+1)}{8\pi^3e^2N_0} \frac{9n}{(n^2+2)^2} \frac{\ln 10}{\lambda L} \int_J^{J'} OD(\lambda) d\lambda \quad (2)$$

where J and J' are the total angular momentum quantum numbers of the initial and final states, h is the Planck constant, c is speed of light, e is the electron charge, N_0 is the concentration of the Dy³⁺ ions, n is the refractive index which is calculated from Ref. [21], L is the thickness of sample, and $OD(\lambda)$ is the optical density, respectively. The theoretical absorption line strength of the electric-dipole transition can be written as Eq. (2):

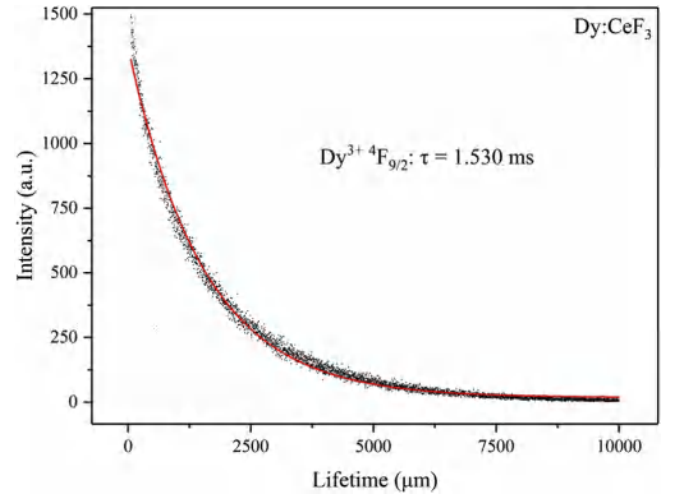


Fig. 5. The measured and fitted Fluorescence decay curves of Dy³⁺:⁴F_{9/2} level.

Table 3

Calculated emission cross-section, radiation transition rates, branching ratios, and the radiation lifetimes for the ⁴F_{9/2} energy level.

Transition ⁴ F _{9/2} →	λ (nm)	σ _{em} (10 ⁻²⁰ cm ²)	A (s ⁻¹)	β (%)	τ _r (ms)
⁶ H _{15/2}	479	0.1735	76.117	28.52	3.747
⁶ H _{13/2}	569	0.9259	169.983	63.70	
⁶ H _{11/2}	660	0.1215	13.462	5.04	
⁶ H _{9/2} + ⁶ F _{11/2}	751	0.1082	7.293	2.73	

$$S_{\text{cal}}^{\text{ed}}(J, J') = \sum_{i=2,4,6} \Omega_i |S, L, JU^{(i)}S', L', J'|^2 \quad (3)$$

Where $U^{(i)}$ is the reduced matrix elements, and it is taken from Ref. [22]. Ω_t ($t=2, 4, 6$) are the J-O intensity parameters. In addition, the

theoretical absorption line strength of the magnetic-dipole transition takes effects only if the transition is satisfied with the transition selection rules: $\Delta S = \Delta L = 0$, $\Delta J = 0/\pm 1$. The S_{exp} and S_{cal} are also listed in Table 1. Through the least-square fitting between S_{exp} and S_{cal} , the three J-O intensity parameters were obtained: $\Omega_2 = 1.01 \times 10^{-20} \text{ cm}^2$, $\Omega_4 = 0.69 \times 10^{-20} \text{ cm}^2$ and $\Omega_6 = 0.91 \times 10^{-20} \text{ cm}^2$, respectively. The J-O intensity parameters comparison of Dy:CeF₃ crystal and other host crystals are given in Table 2. The root-mean-square (RMS) deviation as the measurements of error between the measured and calculation line strengths was calculated by Eq. (4):

$$\text{RMS} = \sqrt{\frac{\sum_{J'} (S_{\text{exp}} - S_{\text{cal}})^2}{N-3}} \quad (4)$$

where N is the number of the transitions. The RMS deviation is $8.4611 \times 10^{-22} \text{ cm}^2$, indicating the J-O intensity parameters is credibility for predicting the luminescent properties of Dy:CeF₃.

Furthermore, using the obtained Ω_t parameters, the spontaneous emission probabilities A ($=A_{\text{ed}} + A_{\text{md}}$) can be calculated by:

$$A_{\text{ed}}(J, J') = \frac{64\pi^4 e^2}{3h(2J+1)\lambda^3} \frac{n(n^2+2)^2}{9} \sum_{i=2,4,6} \Omega_i |S, L, JU^{(i)}S', L', J'|^2 \quad (5)$$

A_{md} takes effects only when the transition follows the transition selection rule. The radiative lifetime.

The fluorescence branching ratios β is defined by:

$$\beta(J, J') = \frac{A(J, J')}{\sum_{J'} A(J, J')} \quad (6)$$

The room temperature emission spectra ranging from 400 to 800 nm of Dy:CeF₃ crystal were measured under excited at 350 nm, shown as emission cross-section with the energy level scheme of Dy³⁺:⁴F_{9/2} emission in Fig. 4. The four emission bands centered at 479 nm, 569 nm, 660 nm and 751 nm were detected, corresponding to the transitions from ⁴F_{9/2} to ⁶H_{15/2}, ⁶H_{13/2}, ⁶H_{11/2} and ⁶H_{9/2} + ⁶F_{11/2}, respectively. The intense 570 nm wavelength shows good emission performance for the yellow fluorescence. The results indicate that the Dy:CeF₃ crystal is a potential candidate for yellow laser operation.

The fluorescence decay curves for the ⁴F_{9/2} multiplet of Dy³⁺ ions in Dy:CeF₃ crystal under pulse excitation of 350 nm is shown in Fig. 5, and τ_f is 1.530 ms, which is much lower than the radiative lifetime τ_r (3.747 ms) calculated by the Judd–Ofelt approach, and the quantum efficiency ($\eta = \tau_f/\tau_r$) reaches to 40.83%. The calculated lifetime τ_r is given as the reciprocal of total radiative probability:

$$\tau_r(J) = \frac{1}{\sum_{J'} A(J, J')} \quad (7)$$

There are two main reasons for the large deviation between τ_f and τ_r : On the one hand, the J–O theory is prone to overestimate the value of the radiative lifetime due to its partial inadequacy in predicting the radiative properties [33]; on the other hand, Bridgeman method of growth crystal increased inside stress and structural defects of the crystal [34], which is further reduces the optical properties of the crystal. Despite this, as far as we know this is the longest fluorescence lifetime of Dy³⁺:⁴F_{9/2} level compared CeF₃ to other host crystals. The longer fluorescence lifetime indicating higher energy storage ability and the higher potential for Q-switched lasers application. The ⁴F_{9/2} fluorescence lifetime comparison of Dy:CeF₃ crystal and other host crystals are also given in Table 2. Unfortunately, due to the absorption of the CeF₃ crystal host in the infrared region, we cannot measure the lower level fluorescence lifetime.

The corresponding stimulated emission cross-section can be calculated according to the Fuchtbauer–Ladenburg theory:

$$\sigma_{\text{em}} = \frac{\lambda^5 I(\lambda) A \beta}{8\pi c \int n^2(\lambda) \lambda I(\lambda) d\lambda} \quad (8)$$

where A is the radiation transition rates, c is the speed of light, $n(\lambda)$ is

the refractive index of light with wavelength λ in the crystal, τ_r is the radiative lifetime of ⁴F_{9/2}, and $I(\lambda)$ refers to the measured fluorescence intensity at wavelength λ . At 570 nm, the peak emission cross-sections are calculated to be $0.9259 \times 10^{-20} \text{ cm}^2$. The high emission cross-sections indicate that Dy:CeF₃ crystal would be available for laser operation in the yellow region. Above all, the emission cross-section, spontaneous emission probabilities, fluorescent branching ratio and radiative lifetimes for different transition levels also shown in Table 3.

4. Conclusion

In conclusion, Dy³⁺-doped CeF₃ crystal was successfully prepared, and a 570 nm emission was obtained in the present fluoride crystal. Compared with other Dy³⁺-doped host crystals, it is found that the Dy:CeF₃ crystal has high emission cross section ($0.9259 \times 10^{-20} \text{ cm}^2$) and longer fluorescence lifetime (1.53 ms) to the stimulated emission of Dy³⁺:⁴F_{9/2} → ⁶H_{13/2} transition. All of the results indicate that the Dy:CeF₃ crystal is a promising material for 570 nm laser applications.

Conflicts of interest

The authors declared that there is no conflict of interest.

Acknowledgment

The experiments were supported by National Key R&D Program of China (No.2016YFB1102302, No.2016YFB0701002), National Natural Science Foundation of China (No.51872307), Equipment Pre-research Foundation Project of China (No.61409220309).

References

- [1] W. Liang, G.C. Sun, X. Yu, et al., All-solid-state Nd: YAG-LBO yellow laser at 572 nm, *Laser Phys.* 21 (6) (2011) 1067.
- [2] Q. Fang, D. Lu, H. Yu, et al., Self-frequency-doubled vibronic yellow Yb: YCOB laser at the wavelength of 570 nm, *Opt. Lett.* 41 (5) (2016) 1002–1005.
- [3] C.K. Sramek, L.S.B. Leung, Y.M. Paulus, et al., Therapeutic window of retinal photocoagulation with green (532-nm) and yellow (577-nm) lasers, *Ophthalmic Surgery, Lasers and Imaging Retina* 43 (4) (2012) 341–347.
- [4] A.A. Kaminskii, J.B. Gruber, S.N. Bagaev, et al., Optical spectroscopy and visible stimulated emission of Dy³⁺ ions in monoclinic α-KY (WO 4) 2 and α-KGd (WO 4) 2 crystals, *Phys. Rev. B* 65 (12) (2002) 125108.
- [5] T.T. Basiev, A.A. Sobol, Y.K. Voronko, et al., Spontaneous Raman spectroscopy of tungstate and molybdate crystals for Raman lasers, *Opt. Mater.* 15 (3) (2000) 205–216.
- [6] S. Nakamura, M. Senoh, S. Nagahama, et al., Blue InGaN-based laser diodes with an emission wavelength of 450 nm, *Appl. Phys. Lett.* 76 (1) (2000) 22–24 666.
- [7] S.R. Bowman, S. O'Connor, N.J. Condon, Diode pumped yellow dysprosium lasers, *Opt. Express* 20 (12) (2012) 12906–12911.
- [8] P.W. Metz, F. Moglia, F. Reichert, et al., Novel rare earth solid state lasers with emission wavelengths in the visible spectral range[C]/2013 Conference on Lasers & Electro-Optics Europe & International Quantum Electronics Conference CLEO EUROPE/IQEC. IEEE, (2013) 1-1.
- [9] G. Bolognesi, D. Parisi, D. Calonico, et al., Yellow laser performance of Dy³⁺ in co-doped Dy, Tb: LiLuF₄, *Opt. Lett.* 39 (23) (2014) 6628–6631.
- [10] A. Bensalah, K. Shimamura, V. Sudesh, et al., Growth of Tm, Ho-codoped YLiF₄ and LuLiF₄ single crystals for eye-safe lasers, *J. Cryst. Growth* 223 (4) (2001) 539–544.
- [11] J. Hong, L. Zhang, Y. Hang, et al., Spectroscopic and thermal characterizations of Yb: LaF₃ single crystal, *Opt. Mater.* 60 (2016) 128–131.
- [12] K. Ahrens, The magnetoelastic interaction of optical phonons in Ce c La 1 – c F 3 single crystals, *Z. Phys. B Condens. Matter* 40 (1) (1980) 45–54.
- [13] D.A. Jones, W.A. Shand, Crystal growth of fluorides in the lanthanide series, *J. Cryst. Growth* 2 (6) (1968) 361–368.
- [14] J. Hong, L. Zhang, Y. Hang, et al., Spectroscopic and thermal characterizations of Yb: LaF₃ single crystal, *Opt. Mater.* 60 (2016) 128–131.
- [15] S. Li, L. Zhang, M. He, et al., Effective enhancement of 2.87 μm fluorescence via Yb³⁺ in Ho³⁺: LaF₃ laser crystal, *J. Lumin.* 203 (2018) 730–734.
- [16] R.A. Buchanan, H.E. Rast, H.H. Caspers, Infrared absorption of Ce³⁺ in LaF₃ and of CeF₃, *J. Chem. Phys.* 44 (11) (1966) 4063–4065.
- [17] B. Liu, J. Shi, Q. Wang, et al., Crystal growth and yellow emission of Dy: YAlO₃, *Opt. Mater.* 72 (2017) 208–213.
- [18] S. Nakamura, M. Senoh, S. Nagahama, et al., Blue InGaN-based laser diodes with an emission wavelength of 450 nm, *Appl. Phys. Lett.* 76 (1) (2000) 22–24.
- [19] B.R. Judd, Optical absorption intensities of rare-earth ions, *Phys. Rev.* 127 (3) (1962) 750.
- [20] G.S. Ofelt, Intensities of crystal spectra of rare-earth ions, *J. Chem. Phys.* 37 (3)

- (1962) 511–520.
- [21] R. Laiho, M. Lakkisto, Investigation of the refractive indices of LaF₃, CeF₃, PrF₃ and NdF₃, *Philos. Mag. B* 48 (2) (1983) 203–207.
- [22] C.K. Jayankar, E. Rukmini, Spectroscopic investigations of Dy³⁺ ions in borosulphate glasses, *Phys. B Condens. Matter* 240 (3) (1997) 273–288.
- [23] A. Lupei, V. Lupei, C. Gheorghe, et al., Spectroscopic characteristics of Dy³⁺ doped Y₃Al₅O₁₂ transparent ceramics, *J. Appl. Phys.* 110 (8) (2011) 083120.
- [24] Y. Wang, Z. You, J. Li, et al., Optical properties of Dy³⁺ ion in GGG laser crystal, *J. Phys. D Appl. Phys.* 43 (7) (2010) 075402.
- [25] B. Liu, J. Shi, Q. Wang, et al., Crystal growth and yellow emission of Dy: YAlO₃, *Opt. Mater.* 72 (2017) 208–213.
- [26] X. Xu, Z. Hu, R. Li, et al., Optical spectroscopy of Dy³⁺-doped CaGdAlO₄ single crystal for potential use in solid-state yellow lasers, *Opt. Mater.* 66 (2017) 469–473.
- [27] E. Cavalli, M. Bettinelli, A. Belletti, et al., Optical spectra of yttrium phosphate and yttrium vanadate single crystals activated with Dy³⁺, *J. Alloy. Comp.* 341 (1–2) (2002) 107–110.
- [28] M.G. Brik, T. Ishii, A.M. Tkachuk, et al., Calculations of the transitions intensities in the optical spectra of Dy³⁺: LiYF₄, *J. Alloy. Comp.* 374 (1–2) (2004) 63–68.
- [29] S. Bigotta, M. Tonelli, E. Cavalli, et al., Optical spectra of Dy³⁺ in KY₃F₁₀ and LiLuF₄ crystalline fibers, *J. Lumin.* 130 (1) (2010) 13–17.
- [30] D. Parisi, A. Toncelli, M. Tonelli, et al., Optical spectroscopy of BaY₂F₈: Dy³⁺, *J. Phys. Condens. Matter* 17 (17) (2005) 2783.
- [31] G.Z. Chen, J.G. Yin, L.H. Zhang, et al., Optical properties of Dy³⁺ ion in PbF₂ laser crystal, *Laser Phys. Lett.* 10 (11) (2013) 115801.
- [32] S. Li, L. Zhang, P. Zhang, et al., Spectroscopic characterizations of Dy: LaF₃ crystal, *Infrared Phys. Technol.* 87 (2017) 65–71.
- [33] S. Bigotta, M. Tonelli, E. Cavalli, et al., Optical spectra of Dy³⁺ in KY₃F₁₀ and LiLuF₄ crystalline fibers, *J. Lumin.* 130 (1) (2010) 13–17.
- [34] M. Shi, J. Xu, Large size LaF₃: Eu: Ca crystal grown by Bridgman–Stockbarger method, *Mater. Lett.* 58 (29) (2004) 3823–3825.